

A MINIATURE, HIGH-SENSITIVITY, ELECTRON TUNNELING ACCELEROMETER

Howard K. Rockstad,* J. K. Reynolds,** T. K. Tang,* T. W. Kenny,**
W. J. Kaiser,*** and Thomas B. Gabrielson****

*Jet Propulsion Laboratory, Center for Space Microelectronics Technology,
California Institute of Technology, Pasadena, CA 91109-8099, USA

**Now at Stanford University, Department of Mechanical Engineering, Stanford, CA 94305-4021, USA

***Now at University of California, Los Angeles, Department of Electrical Engineering,

Los Angeles, CA 90024-1594, USA, and Jet Propulsion Laboratory

****NAWC Aircraft Division, Code 5044, P.O. Box 5152, Warminster, PA 18974-0591, USA

SUMMARY

Prototype low-noise miniature accelerometers have been fabricated with electron-tunneling transducers. The electron-tunneling transducer permits detection of small displacements of the proof mass with high electrical response; such a transducer is essential for a high-performance miniature accelerometer. Prototype accelerometers have shown self-noise of approximately 10^{-7} g per root Hz or less between 10 and 200 Hz, and close to 10^{-8} g per root Hz near the resonant frequency of 100 Hz. Directivity measurements give nulls at least 50 dB below the maximum. A dual-axis prototype designed for underwater acoustic applications is packaged in an 8 cm³ volume with a mass of 8 grams.

INTRODUCTION

Displacement transducers based on electron tunneling have been proposed for a variety of physical sensors, because of the high position sensitivity of electron tunneling. Displacement resolutions approaching 10^{-4} Å/ $\sqrt{\text{Hz}}$ have been shown by Waltman and Kaiser [1] and by Kenny *et al.* [2] for tunnel transducers. Several workers have demonstrated acceleration measurement using electron tunneling transducers. In a device based on a piezoelectric bimorph and a gold wire, Waltman and Kaiser observed an acceleration resolution of 10^{-5} g/ $\sqrt{\text{Hz}}$ with a bandwidth of 3 kHz, where $g = 9.8 \text{ m/s}^2$. Making use of a miniature STM fitted with a 2 gram proof mass, Baski *et al.* [3] observed a resolution better than 10^{-4} g/ $\sqrt{\text{Hz}}$ in a 200 Hz band. Kenny *et al.* [2] used silicon micromachining to fabricate a tunneling accelerometer using a gold-coated silicon tip as a tunneling tip, and a folded cantilever supporting a 30 mg proof mass. An acceleration self-noise of 10^{-7} g/ $\sqrt{\text{Hz}}$ at 10 Hz was inferred from noise measurements [2, 4] on this 200 Hz bandwidth device. Other tunneling accelerometer development activities include that of Zavracky *et al.* [5].

Numerous workers have described other applications for electron tunneling transducers. [6-11] Micromachined silicon accelerometers with μg resolution, not based on electron tunneling, have also been described [12].

We previously described a silicon micromachined dual-element electron tunneling accelerometer design which consists of a proof-mass suspension with a relatively low resonant frequency of 100 Hz or less, and a high-frequency cantilever with a resonant frequency of 5 to 10 kHz [13-15]. A cross-section of this accelerometer is schematically illustrated in Fig. 1. Electron tunneling takes place between a gold-coated silicon tip on the proof mass and a counterelectrode on the high-frequency cantilever. Feedback control is used to maintain constant tunneling current by causing the high-frequency cantilever to closely follow the motion of the proof mass.

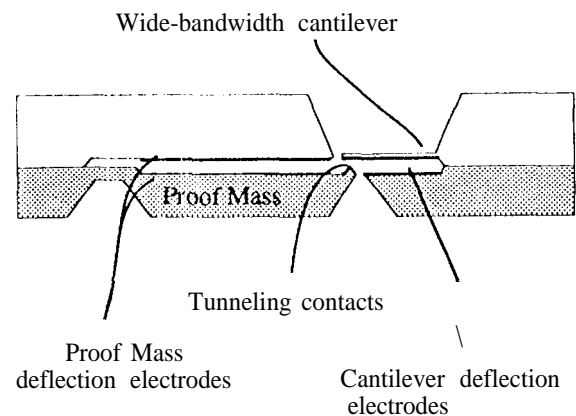


Figure 1. Schematic illustration of the cross-section of the dual-element electron tunneling accelerometer.

Because the feedback control is applied to the high-frequency cantilever, the bandwidth for stable operation is not limited by the resonant frequency of the proof mass suspension; hence, operation from a few Hz to a kHz is readily obtained. Furthermore, the resonant frequency of the proof mass can be chosen to optimize low-frequency

performance, recognizing that low-frequency responsivity of an accelerometer increases as the inverse of the proof-mass resonant frequency squared. Coarse adjustment to bring the tunnel tip within range for tunneling is accomplished by applying a low-pass-filtered feedback voltage to electrostatic deflection electrodes on the proof mass.

in this previous work, mechanical-thermal noise for small masses in a high-performance miniature accelerometer was analyzed and compared with shot and Johnson noise in the electron tunnel circuit [13-16]. It was shown that mechanical-thermal noise for small masses is an important contributor to the self-noise of a high-performance miniature accelerometer. For example, a 100 mg proof mass with a 50 Hz suspension and a Q of 5 contributes about $10^{-8} \text{ g}/\sqrt{\text{Hz}}$ to the accelerometer self-noise, while shot and Johnson noise contribute much less.

PERFORMANCE MODEL

Kenny et al. [2] have measured noise in the tunnel current for gold-coated electrodes, showing a $1/f$ dependence in the noise power, consistent with other measurements [17]. Later current noise measurements, conducted with a gold-coated tip and counterelectrode in a simple configuration and averaged over many measurements were converted to a displacement noise by calibration with a laser vibrometer [18]. These measurements gave rms displacement noise of 6×10^{-3} , 1.5×10^{-3} , and $5 \times 10^{-4} \text{ Å}/\sqrt{\text{Hz}}$ at 10, 100, and 1000 Hz, respectively. We have modeled expected accelerometer self-noise by assuming a $1/\sqrt{f}$ dependence of the displacement noise amplitude as obtained from the above measurements. Displacement noise was converted to a noise-equivalent acceleration through the transfer function:

$$\text{Acceleration} = 4\pi^2 Z \cdot (f_0/f)^2 + f^4/Q^4$$

where Z is the displacement of the proof mass relative to the case, f_0 is the proof-mass resonant frequency, and Q is the mechanical quality factor [15]. A simplified form of the resulting self-noise prediction is illustrated in Fig. 2 for an mQ product of 10-3 kg, corresponding to a 100 mg proof mass and a Q of 10, for example (m is the proof mass). Three cases, for resonant frequencies of 20, 50 and 100 Hz, are shown. Mechanical-thermal noise is also included where it dominates over tunnel transducer noise. As expected from the transfer function, Fig. 2 illustrates that the noise on the high frequency side is independent of resonant frequency, whereas that on the low frequency side can be reduced by reducing the resonant frequency. For a resonant frequency f_0 of 100 Hz, the self-noise is dominated by tunnel transducer noise. For lower resonant frequencies, the contribution of tunnel transducer

noise to equivalent acceleration noise is reduced, and mechanical-thermal noise (horizontal segments in the figure) dominates in a specific frequency band,

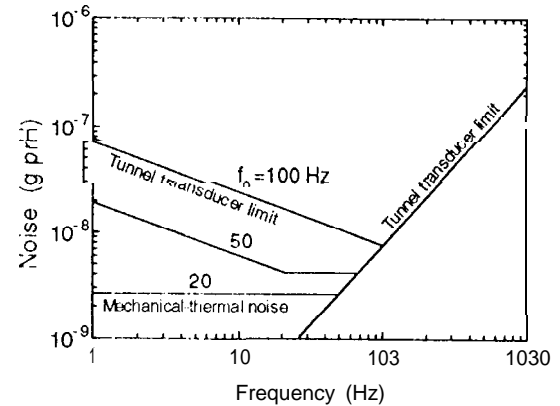


Figure 2. Simplified version of predicted accelerometer self-noise, based on measured displacement noise for micromachined electron tunneling sensors and on theoretical mechanical-thermal noise. Horizontal segments derive from mechanical-thermal noise.

For the parameters chosen and a resonant frequency of 50 Hz, the figure illustrates self-noise less than $10^{-8} \text{ g}/\sqrt{\text{Hz}}$ from 2 to 100 Hz. Further reduction in f_0 brings additional reduction of the low-frequency acceleration noise; however, such reductions in f_0 are accompanied by larger deflections of the mass in a gravitational or other acceleration force field and also by springs more susceptible to fracture.

EXPERIMENTAL

Accelerometers were fabricated with silicon micromachining as described earlier [15]. The accelerometer consists of three components, one containing the high-frequency cantilever, one containing the proof mass, and one forming a stop to prevent large excursions of the proof mass. External dimensions are approximately $1.4 \times 1.2 \times 0.1 \text{ cm}^3$. The proof mass is suspended from one edge in a silicon "hinge" configuration. A metal square of about 60 mg was bonded to the 23 mg silicon proof mass to give the desired mass. A silicon pyramid was etched near the free end of the proof mass and coated with diffusion barrier layers and gold to form the tunnel tip.

Accelerometer responsivity has been determined on two vibration test stations. one station consists of a massive metal plate suspended from a tripod with elastic cords to provide isolation from floor vibration; coupling of horizontal floor vibration is reduced through the pendulum nature of the suspension. The test

accelerometer and a Kistler Piezobeam reference accelerometer were mounted back-to-back, with the test accelerometer mounted in a vacuum chamber attached to the metal plate. The composite was driven by a sinusoidal vibration. Responsivity and directivity were also determined in a standard gradient-hydrophore calibrator. The noise floor was determined in a vacuum-isolation chamber.

Figure 3 shows responsivity vs. frequency for a prototype device with a resonance frequency near 100 Hz. The device in this case is operating in an air pressure of 1 Torr. At this pressure, Q is approximately 5. The low-frequency response is approximately 15 kV/g.

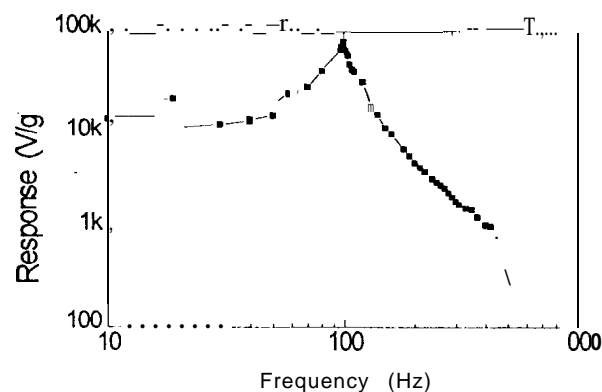


Figure 3. Responsivity vs. frequency.

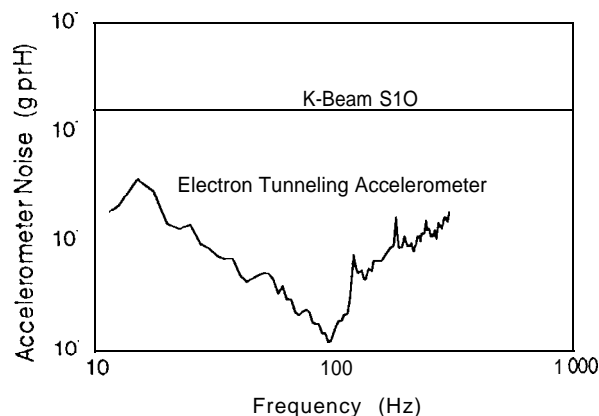


Figure 4. Noise measured for an electron tunnel accelerometer and for a miniature commercial Kistler accelerometer for comparison. The peak near 15 Hz was shown independently to be due to the environment. The tunnel accelerometer data were obtained from a frequency scan; the K-beam data were obtained by averages at selected frequencies.

Figure 4 shows the noise floor measured for this device in a vacuum isolation chamber. The minimum near 90 Hz is near $10^{-8} \text{ g}/\sqrt{\text{Hz}}$. At 10 Hz, the measured noise is $1.5 \times 10^{-7} \text{ g}/\sqrt{\text{Hz}}$. The peak around 15 Hz is due to the environment, as confirmed by independent measurements with other sensors.

Directivity measurements performed in the gradient hydrophore calibrator showed that the nulls perpendicular to the axis of the accelerometer are at least 50 dB below the maxima.

PACKAGING

A dual-axis prototype is packaged in an 8 cm^3 sphere for underwater acoustic applications. Two electron tunneling accelerometers are mounted in quadrature on a cubic frame; hybrid electronic substrates populated with surface-mount components are mounted on two complementary faces of the cubic frame to provide feedback control electronics. The circuit, based on the dual control feedback circuit described earlier [13-14], is revised to reduce power consumption. Quiescent voltages of approximately 100 V and 50 V are applied to the deflection electrodes of the high-frequency cantilever and the proof mass, respectively.

CONCLUSIONS

Miniature dual-element accelerometers based on electron tunneling transducers have been fabricated and tested. Operation over more than a kHz bandwidth, with limiting detectabilities of $10^{-7} \text{ g}/\sqrt{\text{Hz}}$ or better between 10 and 200 Hz, has been demonstrated. Detectability near $10^{-8} \text{ g}/\sqrt{\text{Hz}}$ at 1001 Hz has been demonstrated. Nulls for excitation 90° off-axis are at least 50 dB below the maxima. Predictions based on empirical data for electron tunneling transducers indicate that lower detectabilities, $\sim 10^{-8} \text{ g}/\sqrt{\text{Hz}}$ from several Hz to 100 Hz, for example, are possible. Work is continuing to lower the limiting detectability.

ACKNOWLEDGEMENT

The research described in this paper was performed by the Center for Space Microelectronics Technology, Jet Propulsion Laboratory, California Institute of Technology, and was jointly sponsored by Naval Air Warfare Center, Ballistic Missile Defense Organization/Innovative Science and Technology Office, and Advanced Research Projects Agency, through an agreement with the National Aeronautics and Space Administration.

REFERENCES

- [1] Waltman, S. B.; and Kaiser, W.J. Sensors and Actuators 19(1 989) 201-210.
- [2] Kenny, T. W.; Waltman, S. B.; Reynolds, J. K.; and Kaiser, W.J. Appl. Phys. Lett. 58 (1991) 100-102.
- [3] Baski, A. A.; Albrecht, T. R.; and Quate, C.F. J. Microscopy 157 (1988) 73-76.
- [4] Kenny, T.W.; Kaiser, W. J.; Reynolds, J. K.; Podosek, J. A.; Rockstad, H.K.; Vote, E. C.; and Waltman, S.B. J. Vac. Sci. Technol. A10 (1992) 2114-2118.
- [5] Zavracky, P. M.; Hartley, F.; Sherman, N.; Hansen, 'f.; and Warner, K. Abstr. Late News Papers, The 7th Int. Conf. Solid-State Sensors and Actuators, Transducers '93 (Yokohama, Japan, June 7-10, 1993) pp. 50-51.
- [6] Niksch, M.; and Binnig, G. J. Vac. Sci. Technol. A6 (1988) 470-471.
- [7] Bocko, M. F.; Stephenson, K. A.; and Koch, R.H. Phys. Rev. Lett. 61 (1988) 726-729.
- [8] Wandass, J.I.; Murday, J. S.; and Colton, R.J. Sensors and Actuators 19 (1 989) 211-225.
- [9] Brizzolara, R. A.; Colton, R. J.; Wun-Fogle, M.; and Savage, H.T. Sensors and Actuators 20 (1989) 199-205.
- [10] Brizzolara, R.A.; and Colton, R.J. J. Magn. Mater. 88 (1990) 343-350.
- [11] Kenny, T.W.; Kaiser, W. J.; Waltman, S. B.; and Reynolds, J.K. Appl. Phys. Lett. 59 (1991) 1820-1822.
- [12] Rudolph, F. Sensors and Actuators **A21-A23** (1990) 297-301.
- [13] Rockstad, H. K.; Kenny, T. W.; Reynolds, J. K.; Kaiser, W. J.; VanZandt, T. R.; and Gabrielson, T.B. Digest of Techn. Papers, ASME Winter Annual Meeting, DSC-40, Micromechanical Systems (Anaheim, CA, USA, Nov. 8-13, 1992) pp. 41-52.
- [14] Rockstad, H.K.; Kenny, T. W.; Reynolds, J. K.; Kaiser, W. J.; and Gabrielson, T.B. Digest of Techn. Papers, The 7th Int. Conf. Solid-State Sensors and Actuators, Transducers '93 (Yokohama, Japan, June 7-10, 1993) pp. 836-839.
- [15] *ibid.*, Sensors and Actuators A43 (1994) 107-114.
- [16] Gabrielson, T.B. IEEE Trans. Electron Devices ED-40 (1993) 903-909.
- [17] Abraham, D. W.; Williams, C.C. and Wickramasinghe, H.K. Appl. Phys. Lett. 53 (1988) 1503.
- [18] Kenny, T.W. unpublished.